FGFR1-mediated protocadherin-15 loading mediates cargo specificity during intraflagellar transport in inner ear hair-cell kinocilia

Akira Honda[a,1], Tomoko Kita[a,b,1], Shri Vidhya Seshadri[c], Kazuyo Misaki[d,e], Zamal Ahmed[f], John E. Ladbury[f,g,h], Guy P. Richardson[i], Shigenobu Yonemura[d,e], and Raj K. Ladher[a,c,2]

[a]Laboratory for Sensory Development, RIKEN Center for Developmental Biology, 650-0047 Kobe, Japan; [b]Department of Otolaryngology, Head and Neck Surgery, Kyoto University Hospital, 606-8507 Kyoto, Japan; [c]National Centre for Biological Sciences, 560-065 Bangalore, India; [d]Ultrastructural Research Team, RIKEN Center for Life Science Technologies, 650-0047 Kobe, Japan; [e]Department of Cell Biology, Tokushima University, 770-8503 Tokushima, Japan; [f]School of Molecular and Cellular Biology, University of Leeds, LS2 9JT Leeds, United Kingdom; [g]Department of Biochemistry and Molecular Biology, University of Texas MD Anderson Cancer Center, Houston, TX 77030; [h]Center for Biomolecular Structure and Function, University of Texas MD Anderson Cancer Center, Houston, TX 77030; and [i]Sussex Neuroscience, School of Life Sciences, University of Sussex, BN1 9QG Brighton, United Kingdom

Edited by Marianne Bronner, California Institute of Technology, Pasadena, CA, and approved July 3, 2018 (received for review November 17, 2017)

The mechanosensory hair cells of the inner ear are required for hearing and balance and have a distinctive apical structure, the hair bundle, that converts mechanical stimuli into electrical signals. This structure comprises a single cilium, the kinocilium, lying adjacent to an ensemble of actin-based projections known as stereocilia. Hair bundle polarity depends on kinociliary protocadherin-15 (Pcdh15) localization. Protocadherin-15 is found only in hair-cell kinocilia, and is not localized to the primary cilia of adjacent supporting cells. Thus, Pcdh15 must be specifically targeted and trafficked into the hair-cell kinocilium. Here we show that kinocilial Pcdh15 trafficking relies on cell type-specific coupling to the generic intraflagellar transport (IFT) transport mechanism. We uncover a role for fibroblast growth factor receptor 1 (FGFR1) in loading Pcdh15 onto kinociliary transport particles in hair cells. We find that on activation, FGFR1 binds and phosphorylates Pcdh15. Moreover, we find a previously uncharacterized role for clathrin in coupling this kinocilia-specific cargo with the anterograde IFT-B complex through the adaptor, DAB2. Our results identify a modified ciliary transport pathway used for Pcdh15 transport into the cilium of the inner ear hair cell and coordinated by FGFR1 activity.

inner ear | ciliogenesis | protein trafficking | fibroblast growth factor | signaling

Hair bundles are specialized apical organelles found on mechanosensory hair cells. They are composed of an eccentrically placed cilium, the kinocilium, that lies adjacent to graded, height-ranked rows of actin-based microvilli known as stereocilia (1). Mechanotransduction occurs in stereocilia and relies on filamentous connectors composed of the transmembrane proteins cadherin-23 (Cdh23) and protocadherin-15 (Pcdh15). These tip links bridge the tip of each stereocilium, with the lateral wall of the next tallest (2). For normal function, the hair bundles must be correctly oriented and coaligned with one another throughout the auditory epithelium (3). The planar cell polarity pathway (PCP) ensures this alignment, and the interpretation of PCP cues is mediated through the kinocilia (4). This can be demonstrated in mouse mutants in which hair-cell cilia formation is disrupted and which show defects in the bundle morphogenesis and alignment (4, 5). Polarity also depends on kinocilial links. These, like tip links, are composed of Cdh23, found in the longest stereocilia, and Pcdh15, found in the kinocilium (6–8). Mice lacking Pcdh15 result in a phenotype similar to the loss of cilia showing a disruption of hair bundle morphogenesis and alignment (8). Thus, understanding how Pcdh15 is localized to kinocilia is fundamental to understanding how hair-cell polarity is generated.

Ciliary transport is mediated by multiprotein complexes known as intraflagellar transport (IFT) particles that connect the microtubular axoneme with motor proteins. Anterograde transport into the cilium is mediated by IFT-B particles that associate with kinesin-2, and retrograde transport is mediated by IFT-A particles that associate with dynein. In the inner ear, the involvement of these components in kinocilium formation has been demonstrated using mutant studies. Mutations in components of the IFT complex disrupt kinocilia formation and result in abnormal hair bundle morphology and orientation (5, 9–11). The finding that Pcdh15 mutations are compounded by mutations in the IFT machinery suggests a genetic interaction between the two (8). Moreover, analysis of mice lacking the intracellular domain of the CD2 isoform of Pcdh15 has shown defects in hair bundle development, further suggesting that along with the extracellular interaction with Cdh23, intracellular interactions are also important (12, 13). Proteins that interact with the C-terminal intracellular domain of Pcdh15 have not been identified in kinocilia, leaving open the questions of kinocilial Pcdh15 localization and action.

To understand Pcdh15 localization, in the present study we characterized the components of the Pcdh15 transport machinery in hair-cell kinocilia. We found that the CD2 isoform of Pcdh15 binds the IFT-B complex through an interaction between IFT-57 and the clathrin adaptor, disabled homolog 2 (DAB2), as well as clathrin itself. Importantly, loading of Pcdh15 onto the ciliary transport machinery requires the activity of fibroblast

Significance

Hair cells, the inner ear mechanosensory receptors, are responsible for hearing and balance. This occurs through a specialized apical organelle known as the hair bundle, which is made up of actin-based projections called stereocilia and a microtubule-based kinocilium. These are connected to each other by filaments of proteins composed of cadherin-23 and protocadherin-15 (Pcdh15). Removal of Pcdh15 from the hair cell results in a malformed hair bundle and impacts function. We asked how Pcdh15 is transported into the kinocilium and uncovered a mechanism involving phosphorylation by the fibroblast growth factor receptor 1. Our data suggest a mechanism of hair-cell specialization in which novel interactions enable molecules to enter novel subcellular locations that generate new morphologies and functions.

Author contributions: A.H., T.K., and R.K.L. designed research; A.H., T.K., S.V.S., K.M., Z.A., G.P.R., S.Y., and R.K.L. performed research; A.H., T.K., K.M., Z.A., J.E.L., G.P.R., S.Y., and R.K.L. analyzed data; and A.H., T.K., and R.K.L. wrote the paper.

The authors declare no conflict of interest.

This article is a PNAS Direct Submission.

[1]A.H. and T.K. contributed equally to this work.

[2]To whom correspondence should be addressed. Email: rajladher@ncbs.res.in.

This article contains supporting information online at www.pnas.org/lookup/suppl/doi:10.1073/pnas.1719861115/-/DCSupplemental.

Published online July 30, 2018.

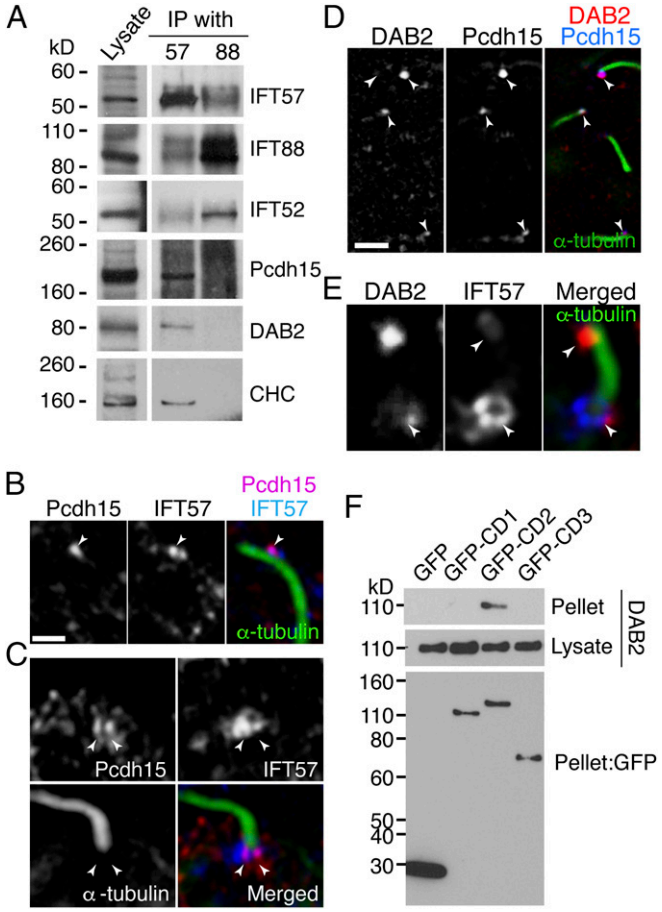

Fig. 1. IFT components bind Pcdh15 in kinocilia. (*A*) IP assay from E10 chick cochlear lysate with anti-IFT57 or anti-IFT88 antibodies. Pcdh15 is cosedimented with IFT57 together with CHC and DAB2. (*B*) Pcdh15 (magenta) and IFT57 (blue) are colocalized in kinocilia (green, stained with anti–α-tubulin antibody) of chick cochlea (BP) at E10 (arrowhead). (*C*) Pcdh15 (red) was colocalized with IFT57 (blue) in the base of kinocilia stained with α-tubulin (green). (*D*) DAB2 (red) and IFT57 (blue) are also colocalized in kinocilia (green) and at the base of the kinocilia. (*E*) DAB2 (magenta) and Pcdh15 (blue) are colocalized in kinocilia (arrowheads) of E10 chick basilar papilla. (Scale bars: 5 μm in *A*, *C*, and *D*; 10 μm in *E*.) (*F*) The GFP-tagged Pcdh15 isoform constructs depicted were coexpressed with DAB2 in BMT10 cells. IP with anti-GFP antibody followed by a DAB2 Western blot shows DAB2 specifically cosediments with the GFP-CD2 domain, but not CD1 or CD3. A GFP Western blot shows similar expression for all tagged isoforms in cells.

growth factor receptor 1 (FGFR1), which phosphorylates the CD2 domain of Pcdh15. Our data describe a model of cargo loading that can lead to cell type-specific ciliary transport necessary for the targeted localization of Pcdh15 to inner ear hair-cell kinocilia.

Results

Protocadherin-15 Interacts with IFT Complex Through DAB2 and Clathrin. Transport into cilia requires loading of protein cargos onto trains of multiprotein IFT complexes (14). We asked whether Pcdh15 interacted with IFT molecules in hair cells. On immunoprecipitation (IP) analysis using embryonic day (E) 10 chick cochlea, we found that Pcdh15 cosedimented with IFT57, but not with IFT88 (Fig. 1*A*). IFT88 is part of the IFT-B1 core complex, whereas IFT57 is part of the IFT-B2 peripheral complex (15). To identify proteins that mediate the interaction of Pcdh15 with IFT57, we used proteomic analysis of the IFT57-IP sample from chick cochlear lysate. We identified clathrin heavy chain (CHC) and light chain, as well as its adaptor, DAB2. These interactions were confirmed using immunolocalization and IP (Figs. 1 *B–D* and 2). Pcdh15 colocalized with IFT57 punctae in kinocilia (Fig. 1*B*). Colocalization was also observed in the kinociliary base. Here IFT57 formed a collar around the kinocilia, whereas Pcdh15 was localized to a subdomain within this region (Fig. 1*C*). DAB2 also colocalized with Pcdh15 in punctae within kinocilia (Fig. 1*D*), and similar to Pcdh15, DAB2 was found in a subdomain of the IFT57 collar at the kinociliary base (Fig. 1*E*).

There are three predominant Pcdh15 isoforms in hair cells, Pcdh15-CD1–3 (12, 13, 16–18), which differ in intracellular domain. Mutant analysis implicates the CD2 isoform in both hair bundle development and mechanotransduction (12, 13). Thus, we asked whether DAB2 preferentially binds one isoform of Pcdh15. We coexpressed DAB2-HA and a partial sequence of mouse Pcdh15 in which the transmembrane and cytoplasmic domains of the CD1–3 isoforms were fused to GFP. Co-IP experiments revealed a specific interaction between DAB2 and Pcdh15-CD2 (Fig. 1*F*). This suggests that DAB2 specifically mediates Pcdh15-CD2 binding to the IFT-B2 complex through an interaction with IFT57.

DAB2 was previously found to be an adaptor for clathrin during receptor-mediated uptake (19). IFT57-IP also identified both CHCs and clathrin light chains. Immunostaining revealed CHC expression in kinocilia of hair cells, as well as localization to the kinociliary base (Fig. 2*A*). In addition to hair-cell kinocilia, CHCs, as well as IFT57 and IFT88, were also detected in primary cilia of supporting cells (SCs), found adjacent to hair cells (Fig. 2*B*). This is in contrast to DAB2, which showed kinocilia-specific localization (Fig. 2*C*), similar to the kinociliary-specific localization of Pcdh15 seen at these stages. Typically, DAB2 mediates clathrin-dependent receptor endocytosis (20) through an interaction with phosphatidylinositol 4,5-bisphosphate, PI(4, 5)P_2 (19, 21). We found that PI(4, 5)P_2 localizes with CHC and Pcdh15 in kinocilia (Fig. 2 *D* and *E*).

Kinociliary Localization of Pcdh15 Requires FGFR1 Activity. To understand how DAB2 recruits a generic IFT pathway for hair-cell

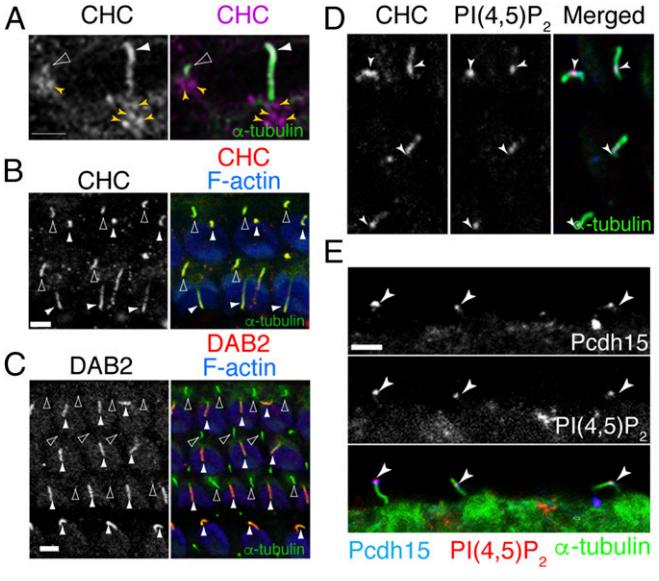

Fig. 2. Clathrin and DAB2 localize to kinocilia. (*A*) SR-SIM imaging shows CHC (magenta) localized in kinocilia (filled arrowheads) and primary cilia (open arrowheads) of sensory epithelia from chick BP at E10, as well as around the periciliary base. (*B*) CHC (magenta) localized in both kinocilia (filled arrowhead) and primary cilia (open arrowhead) of mouse P2 cochlear sensory epithelium. (*C*) DAB2 (red) is localized to kinocilia (filled arrowhead), but not to primary cilia (open arrowhead) of mouse cochlear sensory epithelium at P2. (*D* and *E*) PIP2 showed colocalization with CHC (*D*) and Pcdh15 (*E*) in the kinocilia. Arrowheads highlight colocalization.

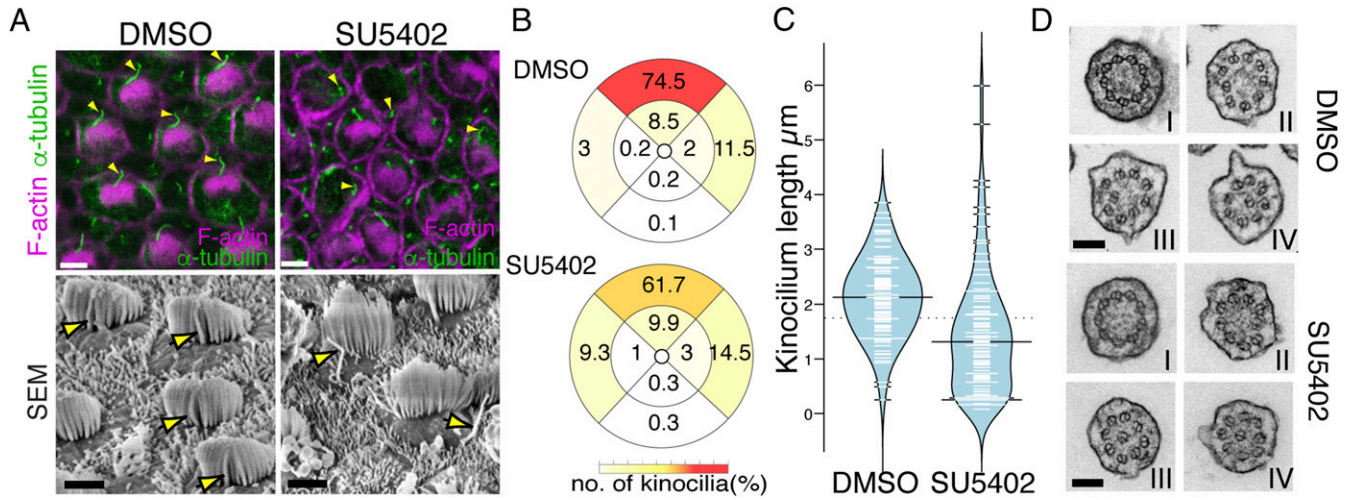

Fig. 3. FGFR1 inhibition results in hair bundle defects. (*A*) E8 chick BP explants were cultured in the presence (SU5402) or absence (DMSO) of SU5402 for 3 d. Immunostaining and SEM data show that the kinocilia exist close to the stereocilia in control samples, but in SU5402 treatment, the kinocilia are separated from the stereocilia bundles (arrowhead). (*B*) Plots showing the percentage of kinocilia found in different regions of the hair cell. Kinocilia position was determined in adjacent hair cells from DMSO- and SU5402-treated E11 chick BP, and the angle deviation was scored into one of nine positions (four explants each, $n = 2,365$ and 2,176, respectively). (*C*) Bean plot showing a reduction in kinocilial length in SU5402-treated hair cells ($n = 100$). (*D*) TEM of cross sections of kinocilia at the base (I), in the middle (II and III), and near the tip (IV) are shown from control and FGFR1-inhibited hair cells. In both case, the axoneme structure was unchanged. (Scale bars: 10 μm in *A*, 0.1 μm in *F*.)

cilia–specific Pcdh15 transport, we took a candidate approach to identify other factors controlling Pcdh15. We had noted that hair bundle polarity in mice mutant for FGFR1 (22) is similar to that in Pcdh15 and Pcdh15-CD2 mutants (12, 13). We thus asked whether inhibition of FGFR1 affects hair bundle formation. FGFR1 has multiple roles during inner ear development necessitating an explant approach to precisely control the timing of FGFR1 inhibition. Chick basilar papilla (BP) was explanted at E8, when hair cells have already been specified but before hair bundle polarization. Isolated sensory epithelia were cultured with either control or the FGFR1 inhibitor SU5402 (23) for 3 d before morphology was assessed (Fig. 3*A*). DMSO (control)-treated epithelia showed normal hair bundle morphology; kinocilia abutted stereocilia, and all hair bundles showed coordinated polarization across the epithelium. In contrast, epithelia treated with SU5402 showed dissociation between the kinocilium and stereocilia, along with a weak hair bundle polarity defect, similar to that observed in Pcdh15 mutants (24) (Fig. 3 *A* and *B*). Measurements of kinocilial length revealed an average size of 2.1 ± 0.7 μm ($n = 100$) in control explants, whereas FGFR1-inhibited kinocilia were smaller (1.4 μm ± 1.1; $n = 100$) (Fig. 3*C*). Previous studies have suggested that ciliogenic genes, such as *Ift88*, are controlled by FGF activity (25, 26). In contrast to these studies, we found that messenger RNA levels of *Ift88*, *Kif3a*, and *Ift57*, as well as protein levels of IFT88 and Kif3a, were unchanged after SU5402 treatment (*SI Appendix*, Fig. S1).

To understand whether FGFR1 inhibition resulted in a change in kinocilial specification, we examined the axoneme. Kinocilia, at least in the early maturation stages, have a divergent axoneme structure. While close to the basal body, the axoneme shows a typical structure of nine microtubule doublets without a central core (a 9 × 2 + 0 configuration); further distal, one doublet deflects inward, giving a distal axoneme morphology of eight doublets surrounding a central doublet (8 × 2 + 1 × 2) (27). Inhibition of FGFR1 did not affect this structure, suggesting that the basic cytoskeletal structure of kinocilia is unaffected (Fig. 3*D*).

The correspondence of the FGFR1 phenotype with the Pcdh15-CD2 mutant (12, 13) prompted us to ask whether Pcdh15 localization is affected by FGFR1 inhibition. In chick hair cells, Pcdh15 is found in distinct punctae decorating the kinocilia. In contrast, kinocilial Pcdh15 was down-regulated after FGFR1 inhibition (Fig. 4*A*). This effect is not due to down-regulation of *Pcdh15* gene transcription, since *Pcdh15* messenger RNA levels were unchanged after SU5402 treatment (Fig. 3*D*). Further examination of kinocilia from SU5402-treated epithelia revealed that although some Pcdh15 could be detected in kinocilia, expression was rarely localized to the kinociliary tips (Fig. 4 *B* and *C*).

FGFR1 Is Localized to Hair-Cell Kinocilia. Our data suggested that FGFR1 activity is necessary for the kinocilial localization of Pcdh15. To determine where FGFR1 could be acting, we next investigated its localization. Immunostaining revealed FGFR1 present as punctae on hair-cell kinocilia of the chick BP (Fig. 5*A*), mouse organ of Corti (Fig. 5*B*), and mouse utricle (Fig. 5*C*). FGFR1 had previously been localized to the nodal cilia of mice, where it participated in establishment of the left-right axis. Here FGFR1 was colocalized with FGFR2 and 3 (28). In contrast, we were unable to detect any ciliary localization of FGFR3 in either hair-cell kinocilia or SC

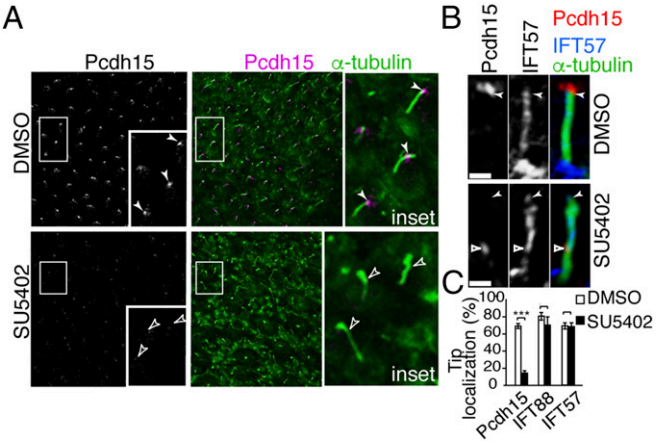

Fig. 4. FGFR1 activity is necessary for kinocilial Pcdh15 localization. (*A*) Kinocilial localization of Pcdh15 was decreased after SU5402 treatment, even though the localization of IFT molecules was unchanged. (*B* and *C*) Superresolution imaging of kinocilia shows that in FGFR1-inhibited hair bundles, Pcdh15 was rarely localized to the tip, although weak expression was detected in the middle of the kinocilia. (Scale bar in *B*: 2 μm.)

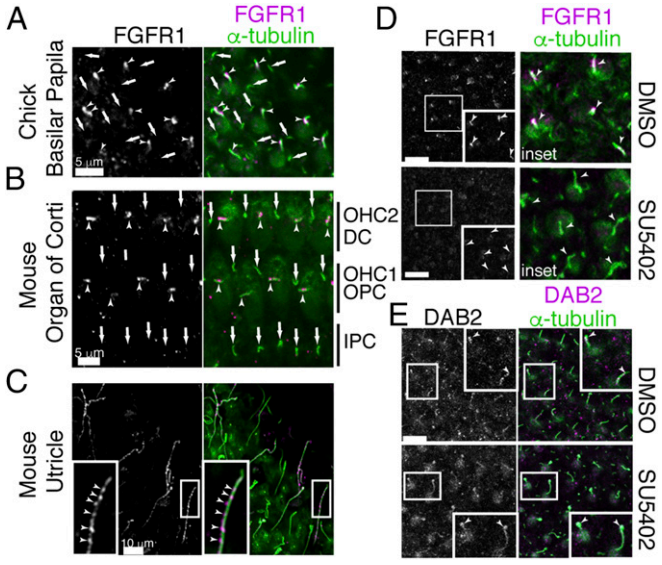

Fig. 5. FGFR1 localizes to the kinocilia. (*A*–*C*) FGFR1 punctae were detected in the kinocilia of E8 chick BP hair cells (*A*), E18.5 mouse cochlea (*B*), and mouse utricle (*C*). Arrowheads and arrows point to kinocilia and primary cilia (green, α-tubulin), respectively. (*D*) SU5402 treatment inhibits FGFR1 kinocilial expression in chick BP. (*E*) SU5402 treatment inhibits DAB2 kinocilial localization in chick BP. (Scale bars: 5 μm in *A* and *B*; 10 μm in *C*–*E*.)

primary cilia, despite its expression in sensory epithelia (29) (*SI Appendix*, Fig. S2). To ask whether FGFR1 kinociliary localization was under FGFR1 control, we treated explanted E8 chick basilar papillae with SU5402. While DMSO controls show good kinocilial FGFR1 localization, the inhibition of FGF signaling results in diminished FGFR1 in kinocilia (Fig. 5*D*).

Having established that FGFR1 is localized to the kinocilia, we next asked whether FGFR1 binds components of the trafficking system. Immunoprecipitation with either IFT88 or IFT57 antibodies failed to detect FGFR1 in the pellet, indicating that FGFR1 did not bind to components of the constitutive IFT machinery (*SI Appendix*, Fig. S3). Consistent with this finding, kinocilial and primary cilial localization of IFT88 or IFT57 was unaffected in SU5402-treated sensory explants (*SI Appendix*, Fig. S3). Similarly, DAB2 localization to kinocilia was unaffected in FGFR-inhibited explants (Fig. 5*E*). However, colocalization of DAB2 and FGFR1 was observed (Fig. 6*A*), suggesting an interaction between these two proteins. Using a co-IP assay, we found that DAB2 binds to FGFR1 independent of FGFR1 activity (Fig. 6*B*). Grb2, which binds FGFR1 through the FGF receptor substrate protein (FRS), has been identified as a binding partner of DAB2 (30). We found that an FGFR1 mutant construct lacking the FRS-binding motif (ΔFBD) was still able to bind DAB2, at levels comparable to the wild-type (WT) FGFR1 construct (Fig. 6*C*). A deletion construct lacking the entire intracellular tyrosine kinase domain was unable to bind DAB2 (Fig. 6*C*).

FGFR1 Binds and Phosphorylates Pcdh15. Despite the inability of FGFR1 to regulate both IFT and DAB2 localization, it is still required for kinociliary localization of Pcdh15. We also observed that FGFR1, Pcdh15, and DAB2 showed colocalization with the kinesin-2 subunit Kif3a in mouse utricular kinocilia (*SI Appendix*, Fig. S4). We thus asked whether FGFR1 can interact with Pcdh15. Pcdh15 colocalized with FGFR1 around the ciliary tip, although minor colocalization punctae were also detected in other regions of the kinocilia (Fig. 7*A*). IP of chick BP lysate revealed FGFR1 cosedimented with Pcdh15 (Fig. 7*B*). This interaction was confirmed using co-IP. HEK293T cells were cotransfected with an HA-tagged construct of FGFR1 together with Pcdh15. Anti-Pcdh15 antibody was used to pellet potential interacting proteins from the cell lysate, and FGFR1 was detected in this pellet. This interaction was abrogated when the cells were treated with SU5402, suggesting that the Pcdh15–FGFR1 interaction requires receptor activation. In addition, we noted FGFR1-dependent tyrosine phosphorylation of Pcdh15 (Fig. 7*C*). As this result was unexpected, we used site-directed mutagenesis to confirm that phosphorylation plays a role in FGFR1–Pcdh15 interaction. The CD2 intracellular region of Pcdh15 has 12 tyrosine residues that are potential substrates for kinases. We generated two mutant Pcdh15 constructs in which either the N-terminal (6F-a) or C-terminal (6F-b) six tyrosines were mutated to phenylalanine. In vitro binding assays revealed that phosphorylation was reduced in these mutants, and neither showed interaction with FGFR1 (Fig. 7*D*). This suggests that tyrosine phosphorylation of the intracellular domain of Pcdh15 facilitates complex formation with FGFR1.

To investigate whether this interaction is direct, we used fluorescence lifetime imaging microscopy (FLIM) to measure fluorescence resonance energy transfer (FRET) between fluorophore-tagged FGFR1 (tagged with GFP) and Pcdh15-CD2 (tagged with mCherry) (Fig. 7*E*). HEK293T cells overexpressing FGFR1-GFP and the Pcdh15-mCherry constructs (WT, 6F-a, and 6F-b) were analyzed. In control cells expressing FGFR1-GFP and mCherry alone, the average lifetime was centered on approximately 2.1 ns. In contrast, in FGFR1-GFP and WT-Pcdh15-mCherry, a population of molecules had a shorter average lifetime of 1.9 ns, seen as a left shift in the peak, indicating direct interactions. The 6F-a mutant showed very limited number of interacting clusters, while the 6F-b completely abrogated all interactions. These results suggest that FGFR1 binds Pcdh15 directly, and that the phosphorylation of Pcdh15 is involved in the formation of a stable Pcdh15–FGFR1 complex.

We next asked whether the FGFR1 activity was required for the binding of Pcdh15 to DAB2. Using our cell line assay system, we transfected FGFR1-HA, DAB2-GFP, and either Pcdh15-FLAG or

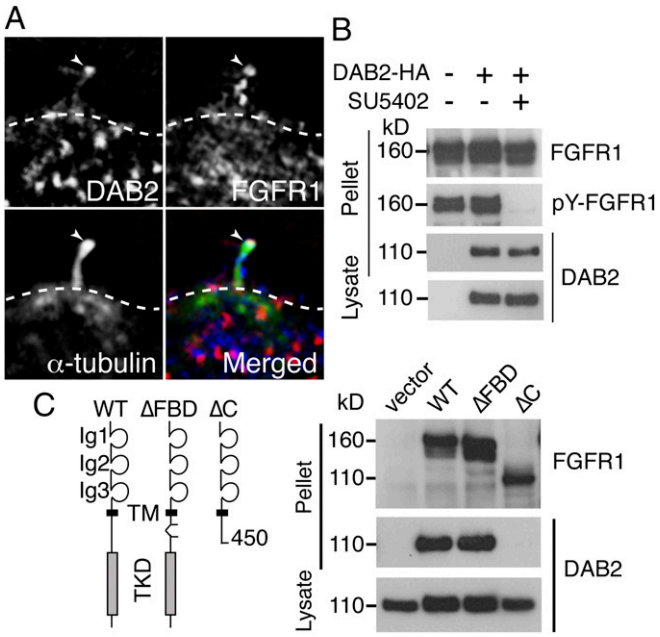

Fig. 6. DAB2 binds FGFR1 independently of FGFR1 activity. (*A*) DAB2 (red) and FGFR1 (blue) were colocalized in the tip of kinocilia (arrowheads). (*B*) IP of DAB2-HA pulled down FGFR1, independently of FGFR1 activity, in overexpressing BMT-10 cells. (*C*) FGFR1 mutant construct, lacking the FRS-binding motif (ΔFBD construct), was still able to bind DAB2 at the same levels as in WT FGFR1 in an in vitro binding assay. An FGFR1 construct lacking the intracellular domain (ΔC construct) was unable to bind DAB2, however.

DEVELOPMENTAL BIOLOGY

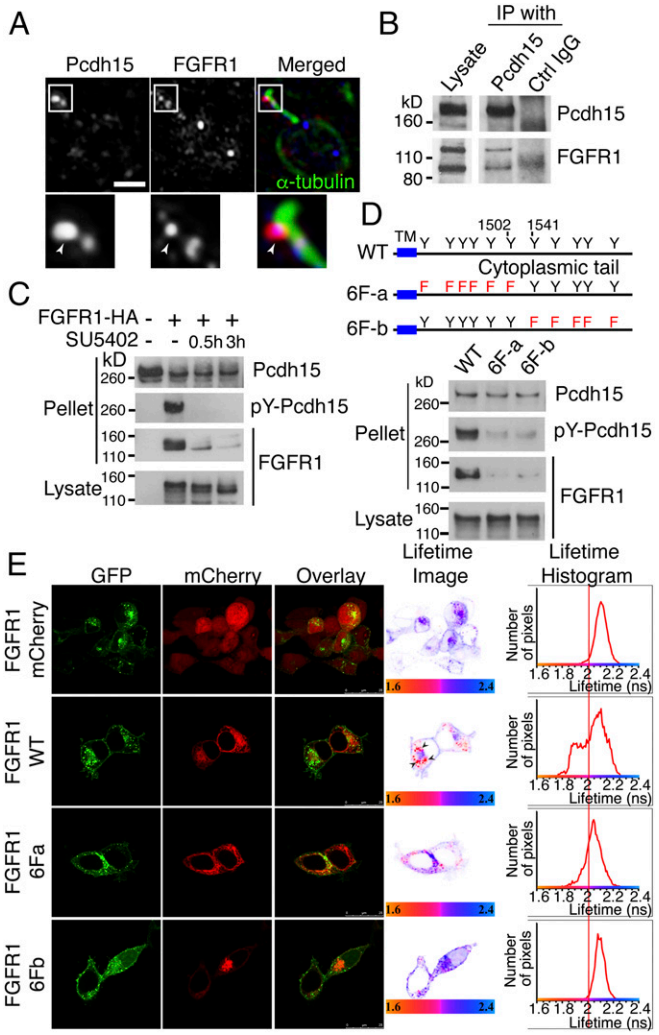

Fig. 7. FGFR1 binds to Pcdh15. (*A*) Pcdh15 (red) and FGFR1 (blue) colocalize in the kinocilia of hair cells of the E9 chick BP (arrowhead). (*B*) FGFR1 cosedimented from chick cochlear lysate after IP with an anti-Pcdh15 antibody. (*C*) Co-IP binding assay using HEK293T cells transfected with HA-tagged FGFR1 and Pcdh15 and cultured in the presence or absence of SU5402. HA IP pulled down Pcdh15 in an FGFR1 activity-dependent manner. Reblotting with a phosphotyrosine antibody showed that Pcdh15 was phosphorylated by FGFR1 activity. (*D*) In vitro binding assay of two nonphosphorylatable Pcdh15-CD2 mutants, 6F-a and 6F-b. Compared with the WT construct, the 6F-a and 6F-b mutants showed a requirement for Pcdh15 phosphorylation in an FGFR1 interaction. (*E*) FRET-FLIM using HEK293T cells overexpressing FGFR1-GFP and Pcdh15-mCherry constructs (WT, 6F-a, and 6F-b) indicate direct interactions observed in intracellular vesicles between FGFR1 and PCdh15. The 6F-a mutant showed very limited number of FGFR1-interacting clusters, while the 6F-b mutant completely abrogated all binding.

Pcdh15-6Fa-FLAG. These were cultured in the presence or absence of SU5402. We found that SU5402 treatment partially abrogated the binding of Pcdh15 to DAB2. No binding of Pcdh15-6Fa to DAB2 was detected (*SI Appendix*, Fig. S5*A*). To understand how DAB2 binds to FGFR1 and Pcdh15, we used a series of DAB2 deletion mutants to investigate which domain was responsible for the FGFR1–Pcdh15 interaction. Both FGFR1 and Pcdh15 were found to bind to the PTB domain of DAB2 (*SI Appendix*, Fig. S5 *B–D*).

Discussion

Pcdh15 is expressed in both hair cells and supporting cells (12, 31), and even though IFT-B particles are found in both types of cilia, the transport of Pcdh-15 is restricted to the hair-cell kinocilia. Our results show that hair-cell–specific kinociliary transport comes from the specific interaction of Pcdh15-CD2 with DAB2, mediated by FGFR1. It is possible that phosphorylation of Pcdh15-CD2 by FGFR1 loads Pcdh15-CD2 onto DAB2, thereby hitching the DAB2–FGFR1–Pcdh15 complex onto IFT-B particles via clathrin. Where this interaction is initiated is unclear, however. Our results identify a role for clathrin in kinocilia transport. Previous studies have shown the accumulation of endocytic components, including clathrin, at the base of cilia (32, 33). Thus, it is possible that vesicles containing clathrin/DAB2/Pcdh15 and FGFR1 are generated in the hair-cell soma and are routed to the kinocilium, similar to what is observed for cadherin-23 and harmonin in zebrafish hair cells (34). However, we detected very few FGFR1/Pcdh15-coexpressing vesicles in the developing hair-cell soma. It is more likely that these proteins arrive separately at the kinocilial base. Once there, FGFR1, Pcdh15, and DAB2 are able to interact, and this interaction enables their coupling onto the IFT machinery for transport into the kinocilium.

DAB2 was identified by virtue of its robust binding to IFT57 in chick cochlear lysate. DAB2 also has been shown to connect the Huntingtin interacting protein, HIP1 (35), which in turn binds IFT57 (36). We were unable to detect HIP1 or the AP-2 clathrin adaptor after pull-down with IFT57 from the chick cochlear lysate (*SI Appendix*, Fig. S6), suggesting that only DAB2 mediates Pcdh15 through clathrin. This interaction is mediated through the phosphoinositide PI(4, 5)P_2. In primary cilia, PI(4, 5)P_2 is restricted to the ciliary base, and the action of an inositol 5-phosphate, INPP5E, generates PI4P, which localizes to the cilium. This restriction has been shown to play an important role in the regulation of hedgehog (Hh) signaling (37, 38). In mice mutant for INPP5E, PI(4, 5)P_2 is found in the cilium. Its localization is also associated with the localization of an attenuator of Hh signaling, Gpr161, which occurs through interactions among PI(4, 5)P_2, its binding protein Tulp3, and the IFT-A complex (37, 38). It is possible that during their differentiation, sensory progenitors exhibit altered activity of inositol phosphatases. In hair cells, this derived condition enables the translocation of PI(4, 5)P_2 into the kinocilium, thereby enabling the interaction of DAB2, clathrin, and IFT57.

The DAB2/clathrin/IFT-B transport particles are necessary for the translocation of Pcdh15 into the kinocilia. Hair cells in which FGFR1 is inhibited show defects reminiscent of Pcdh15-CD2 mutant mice (12, 13), with a mild disruption in planar cell polarity, a decoupling of the kinocilia from stereocilia, but relatively normal stereocilia elongation. Our data also show that FGFR1-mediated Pcdh15 transport phosphorylates the CD2 domain of Pcdh15. This finding emphasizes the importance of the intracellular CD2 domain in hair bundle development. Pcdh15 phosphorylation may recruit other phosphotyrosine-interacting proteins that may mediate the function of Pcdh15 in organizing hair bundle polarity. The CD2 intracellular domain also has a role in mechanotransduction, and it will be of interest to examine the possible role of Pcdh15 phosphorylation in actin-based stereocilia. Indeed, DAB2, in conjunction with an already bound cargo, causes the dimerization and activation of myosin VI (39–41), a myosin associated with hearing loss (42). Although myosin VI is a motor directed to the minus end of actin filaments, cargo-mediated dimerization has been also suggested as a mode of activation for the plus-motors myosin VII and myosin X (41). It would be of interest to determine whether Pcdh15 is phosphorylated in stereocilia, and whether this phosphorylation is also associated with DAB2 and clathrin binding into a complex with myosin VII or myosin X for transport to form tip links.

Methods

Animals. Fertilized chicken eggs were purchased from Shiroyama Farm, Kagawa, Japan and incubated in a humidified incubator at 38 °C until the desired stage. Mice were housed in environmentally controlled rooms at the RIKEN Center for Developmental Biology in accordance with the institutional guidelines for animal experiments.

Antibodies. Anti-chick FGFR1 and anti-chick FGFR3 antibodies were produced as described in *SI Appendix, Methods* and Fig. S7). Mouse mAbs against Pcdh15 have been described elsewhere (17, 43, 44). The following primary antibodies were also used: mouse mAbs against acetylated-tubulin (Sigma-Aldrich); Kif3a, GM130, and CHC (BD Biosciences); phosphotyrosine and CHC (Millipore); PIP2 (Echelon); GFP (Roche); and HA (Covance); rabbit polyclonal Abs (pAbs) against IFT52, IFT57, IFT88, and DAB2 (Proteintech); Pcdh15 (Novus); FGFR1 (Sigma-Aldrich); and DsRed (Clontech); and goat pAbs against DAB2 (Abcam). Anti-chick FGFR1 and anti-chick FGFR3 antibodies were produced as described in *SI Appendix, Methods* and Fig. S7.

Chick BP Explant Culture and SU5402 Treatment. BP was dissected from chick E8 embryos and opened to expose the luminal surface. The explant was placed on a cell culture insert (Falcon) and then incubated in DMEM with 100 U/mL penicillin at 5% CO_2 and 37 °C. To inhibit FGFR activity, 40 μM SU5402 (Calbiochem) was added, and the explants were incubated for 1 or 3 d.

IP and Western Blot Analysis. Cochleae or cells were homogenized. Proteins in samples were separated by 5–20% SDS/PAGE (Wako) and transferred to PVDF membranes. Complete, uncropped, blots are provided in *SI Appendix*, Fig. S8.

DNA Constructs. C-terminally HA-tagged FGFR1, was constructed by subcloning full-length human FGFR1 into a pCAG-HA (45) vector. FGFR1-GFP has been described elsewhere (46). A full-length Pcdh15-CD2 sequence was subcloned into a pCA-SalI-FLAG (47) or pCAG-mCherry (45) vector.

FLIM Analysis. Cells were imaged with a Leica SP5 II confocal microscope. FLIM experiments were performed as described previously (46), and samples were excited with a tunable femtosecond titanium-sapphire pumped laser (Mai Tai BB; Spectra-Physics).

Mass Spectrometry. Affinity-purified proteins were resolved by 5–20% SDS/PAGE (Wako). After silver staining, the protein bands were excised from the gel and subjected to in-gel digestion. The molecular masses of the resulting peptides were compared against the nonredundant National Center for Biotechnology Information database using the MASCOT program.

TEM Analysis. Chick cochleae were dissected, and the surrounding tissues were removed from the cochleae to expose the sensory epithelia before fixation. For TEM analysis, fixed samples, embedded in Poly/Bed 812 (Polyscience) were cut with a diamond knife and then double-stained with uranyl acetate and lead citrate.

ACKNOWLEDGMENTS. We thank Hitoshi Niwa and Masatoshi Takeichi for plasmids, Rieko Nakagawa for mass spectroscopy support, and Junichi Nakayama for advice. We are also grateful to past and present members of the R.K.L. laboratory in Japan and India for technical assistance and discussions. This work was supported by Japan Society for the Promotion of Science KAKENHI Grants JP24592572 and JP25462638, a RIKEN Center for Developmental Biology intramural grant, an Action on Hearing Loss international project grant, and National Centre for Biological Sciences-Tata Institute of Fundamental Research funding from the Indian Department of Atomic Energy.

1. Schwander M, Kachar B, Müller U (2010) Review series: The cell biology of hearing. *J Cell Biol* 190:9–20.
2. Beurg M, Fettiplace R, Nam JH, Ricci AJ (2009) Localization of inner hair cell mechanotransducer channels using high-speed calcium imaging. *Nat Neurosci* 12:553–558.
3. Jones C, Chen P (2008) Primary cilia in planar cell polarity regulation of the inner ear. *Curr Top Dev Biol* 85:197–224.
4. May-Simera HL, Kelley MW (2012) Cilia, Wnt signaling, and the cytoskeleton. *Cilia* 1:7.
5. Jones C, et al. (2008) Ciliary proteins link basal body polarization to planar cell polarity regulation. *Nat Genet* 40:69–77.
6. Raphael Y, et al. (2001) Severe vestibular and auditory impairment in three alleles of Ames waltzer (av) mice. *Hear Res* 151:237–249.
7. Goodyear RJ, Forge A, Legan PK, Richardson GP (2010) Asymmetric distribution of cadherin 23 and protocadherin 15 in the kinocilial links of avian sensory hair cells. *J Comp Neurol* 518:4288–4297.
8. Chacon-Heszele MF, Ren D, Reynolds AB, Chi F, Chen P (2012) Regulation of cochlear convergent extension by the vertebrate planar cell polarity pathway is dependent on p120-catenin. *Development* 139:968–978.
9. May-Simera HL, et al. (2015) Ciliary proteins Bbs8 and Ift20 promote planar cell polarity in the cochlea. *Development* 142:555–566.
10. Abdelhamed ZA, et al. (2015) The Meckel-Gruber syndrome protein TMEM67 controls basal body positioning and epithelial branching morphogenesis in mice via the non-canonical Wnt pathway. *Dis Model Mech* 8:527–541.
11. Okamoto S, et al. (2017) Ick ciliary kinase is essential for planar cell polarity formation in inner ear hair cells and hearing function. *J Neurosci* 37:2073–2085.
12. Webb SW, et al. (2011) Regulation of PCDH15 function in mechanosensory hair cells by alternative splicing of the cytoplasmic domain. *Development* 138:1607–1617.
13. Pepermans E, et al. (2014) The CD2 isoform of protocadherin-15 is an essential component of the tip-link complex in mature auditory hair cells. *EMBO Mol Med* 6:984–992.
14. Lechtreck KF (2015) IFT-cargo interactions and protein transport in cilia. *Trends Biochem Sci* 40:765–778.
15. Taschner M, et al. (2016) Intraflagellar transport proteins 172, 80, 57, 54, 38, and 20 form a stable tubulin-binding IFT-B2 complex. *EMBO J* 35:773–790.
16. Alagramam KN, et al. (2007) Promoter, alternative splice forms, and genomic structure of protocadherin 15. *Genomics* 90:482–492.
17. Ahmed ZM, et al. (2006) The tip-link antigen, a protein associated with the transduction complex of sensory hair cells, is protocadherin-15. *J Neurosci* 26:7022–7034.
18. Ahmed ZM, et al. (2008) Gene structure and mutant alleles of PCDH15: Nonsyndromic deafness DFNB23 and type 1 Usher syndrome. *Hum Genet* 124:215–223.
19. Morris SM, Cooper JA (2001) Disabled-2 colocalizes with the LDLR in clathrin-coated pits and interacts with AP-2. *Traffic* 2:111–123.
20. Tao W, Moore R, Smith ER, Xu XX (2016) Endocytosis and physiology: Insights from disabled-2–deficient mice. *Front Cell Dev Biol* 4:129.
21. Spudich G, et al. (2007) Myosin VI targeting to clathrin-coated structures and dimerization is mediated by binding to Disabled-2 and PtdIns(4,5)P2. *Nat Cell Biol* 9:176–183.
22. Ono K, et al. (2014) FGFR1-Frs2/3 signalling maintains sensory progenitors during inner ear hair cell formation. *PLoS Genet* 10:e1004118.
23. Mohammadi M, et al. (1997) Structures of the tyrosine kinase domain of fibroblast growth factor receptor in complex with inhibitors. *Science* 276:955–960.
24. Kikkawa YS, Pawlowski KS, Wright CG, Alagramam KN (2008) Development of outer hair cells in Ames waltzer mice: Mutation in protocadherin 15 affects development of cuticular plate and associated structures. *Anat Rec (Hoboken)* 291:224–232.
25. Neugebauer JM, Amack JD, Peterson AG, Bisgrove BW, Yost HJ (2009) FGF signalling during embryo development regulates cilia length in diverse epithelia. *Nature* 458:651–654.
26. Hong SK, Dawid IB (2009) FGF-dependent left-right asymmetry patterning in zebrafish is mediated by Ier2 and Fibp1. *Proc Natl Acad Sci USA* 106:2230–2235.
27. Sobkowicz HM, Slapnick SM, August BK (1995) The kinocilium of auditory hair cells and evidence for its morphogenetic role during the regeneration of stereocilia and cuticular plates. *J Neurocytol* 24:633–653.
28. Tanaka Y, Okada Y, Hirokawa N (2005) FGF-induced vesicular release of sonic hedgehog and retinoic acid in leftward nodal flow is critical for left-right determination. *Nature* 435:172–177.
29. Hayashi T, Cunningham D, Bermingham-McDonogh O (2007) Loss of Fgfr3 leads to excess hair cell development in the mouse organ of Corti. *Dev Dyn* 236:525–533.
30. Xu XX, Yi T, Tang B, Lambeth JD (1998) Disabled-2 (Dab2) is an SH3 domain-binding partner of Grb2. *Oncogene* 16:1561–1569.
31. Alagramam KN, et al. (2001) Mutations in the novel protocadherin PCDH15 cause Usher syndrome type 1F. *Hum Mol Genet* 10:1709–1718, and correction (2001) 10:2603.
32. Kaplan OI, et al. (2012) Endocytosis genes facilitate protein and membrane transport in *C. elegans* sensory cilia. *Curr Biol* 22:451–460.
33. Molla-Herman A, et al. (2010) The ciliary pocket: An endocytic membrane domain at the base of primary and motile cilia. *J Cell Sci* 123:1785–1795.
34. Blanco-Sánchez B, Clément A, Fierro J, Jr, Washbourne P, Westerfield M (2014) Complexes of Usher proteins preassemble at the endoplasmic reticulum and are required for trafficking and ER homeostasis. *Dis Model Mech* 7:547–559.
35. Mishra SK, et al. (2002) Disabled-2 exhibits the properties of a cargo-selective endocytic clathrin adaptor. *EMBO J* 21:4915–4926.
36. Gervais FG, et al. (2002) Recruitment and activation of caspase-8 by the huntingtin-interacting protein Hip-1 and a novel partner Hippi. *Nat Cell Biol* 4:95–105.
37. Garcia-Gonzalo FR, et al. (2015) Phosphoinositides regulate ciliary protein trafficking to modulate hedgehog signaling. *Dev Cell* 34:400–409.
38. Chávez M, et al. (2015) Modulation of ciliary phosphoinositide content regulates trafficking and sonic hedgehog signaling output. *Dev Cell* 34:338–350.
39. Morris SM, et al. (2002) Myosin VI binds to and localises with Dab2, potentially linking receptor-mediated endocytosis and the actin cytoskeleton. *Traffic* 3:331–341.
40. Phichith D, et al. (2009) Cargo binding induces dimerization of myosin VI. *Proc Natl Acad Sci USA* 106:17320–17324.
41. Yu C, et al. (2009) Myosin VI undergoes cargo-mediated dimerization. *Cell* 138:537–548.
42. Friedman TB, Sellers JR, Avraham KB (1999) Unconventional myosins and the genetics of hearing loss. *Am J Med Genet* 89:147–157.
43. Goodyear RJ, Richardson GP (2003) A novel antigen sensitive to calcium chelation that is associated with the tip links and kinocilial links of sensory hair bundles. *J Neurosci* 23:4878–4887.
44. Richardson GP, Bartolami S, Russell IJ (1990) Identification of a 275-kD protein associated with the apical surfaces of sensory hair cells in the avian inner ear. *J Cell Biol* 110:1055–1066.
45. Niwa H, Yamamura K, Miyazaki J (1991) Efficient selection for high-expression transfectants with a novel eukaryotic vector. *Gene* 108:193–199.
46. Ahmed Z, et al. (2010) Direct binding of Grb2 SH3 domain to FGFR2 regulates SHP2 function. *Cell Signal* 22:23–33.
47. Nakao S, Platek A, Hirano S, Takeichi M (2008) Contact-dependent promotion of cell migration by the OL-protocadherin-Nap1 interaction. *J Cell Biol* 182:395–410.